Front. Optoelectron. China 2011, 4(2): 161–165
DOI 10.1007/s12200-011-0153-x

RESEARCH ARTICLE

Synthesis and optoelectronic properties of silver-doped n-type CdS nanoribbons

Chunyan WU, Li WANG, Zihan ZHANG, Xiwei ZHANG, Qiang PENG, Jiajun CAI, Yongqiang YU, Huier GUO, Jiansheng JIE (✉)

School of Electronic Science and Applied Physics, Hefei University of Technology, Hefei 230009, China

Abstract Sliver doped n-type CdS nanoribbons (NRs) were successfully synthesized by using Ag_2S as the dopant via a thermal co-evaporation method. The CdS:Ag NRs have wurtzite single-crystal structure with growth direction of [110]. Significantly, the conductivity of the CdS NRs increased ~6 orders of magnitude by silver doping. Moreover, the Ag doped CdS NRs showed much enhanced photoconductivity compared with the undoped ones, which will greatly favor the application of CdS nanostructures in high-performance nano-optoelectronic devices.

Keywords CdS nanoribbons, silver doping, nanodevices, nano-field effect transistors, photoconductivity

1 Introduction

In recent years, one-dimensional (1D) semiconductor 1D nanostructures, such as nanowires (NWs), nanoribbons (NRs), and nanotubes (NTs), have aroused a great deal of interest because of their unique electronic and optical properties arising from quantum confinement and the potential applications in functional nanodevices, such as transistors [1], light emission diodes (LEDs) [2], sensors [3], and photodetectors [4]. Among them, 1D nanostructures of nanoribbons was charactered with a high aspect ratio of both width and length to thickness, which may represent an important building block for nanoscale devices [5].

CdS is one of the most important II-VI group semiconductor materials with a wide direct band gap of 2.42 eV in the visible range at 300 K. CdS nanostructures possess some unique properties such as tuning emission in the visible range [6], excellent photoconductive characteristics [7], and adjustable band gap (1.70–3.68 eV) by alloying with other II-VI compounds, e.g., CdS_xSe_{1-x}, $Zn_xCd_{1-x}S$, and $Zn_xCd_{1-x}Se$ [8]. So far, CdS nanostructures have been extensively used in diverse nano-electronics and nano-optoelectronics devices [9], including optical- and electrical-driven laser emissions [10], high-performance nano-field-effect transistors (nano-FETs) [11,12] and nano-photoswitches [13].

CdS itself is a non-stoichiometric n-type semiconductor. Its n-type characteristic was mainly determined by the small amount of intrinsic donor defects such as S vacancies and Cd interstitials in it. However, unintentionally doped CdS nanostructures are normally highly insulative, which will inevitably hinder their applications in nano-optoelectronic devices. Doping plays a critical role in tuning the optical and electrical properties of semiconductors in the potential applications. Indeed, different dopants, such as In, Cl, Ag, etc. were successfully used for n-type doping in CdS thin films with various methods such as thermal evaporation [14], post-annealing [15], and ion exchange [16]. Among them Ag has attracted much attention due to the interesting phenomena induced by Ag doping, such as the significant shift of the photosensitivity and the increase of the photoresponse in CdS [17]. What's more, Ag doping also provides a convenient way to tailor the physical properties, including photoluminescence (PL) and photocatalysis properties, of various semiconductors [18,19]. Ag doped CdS nanoparticles have been found to manifest strong optical limiting effects [20]. Although many efforts have been made to synthesize 1D CdS nanostructures with different morphologies and structures, Ag doping on CdS 1D nanostructures remains a big challenge and has not been reported so far.

Herein, we reported the *in situ* Ag doping of single-crystal CdS NRs by using Ag_2S as the n-type dopant via thermal co-evaporation method. Electrical measurements conducted on the single CdS:Ag NR revealed that the transport properties of the CdS NRs could be easily

Received October 10, 2010; accepted November 15, 2010

E-mail: jason.jsjie@gmail.com

controlled by Ag doping, thus offering the opportunities to construct high-performance nano-optoelectronic devices based on the CdS:Ag NRs.

2 Experimental details

Silver doping of CdS NRs was carried out in a conventional tube furnace with a horizontal alumina tube, which has two independent heating zones. In a typical experiment, the mixture of 0.25 g CdS powder (99.99%, Aldrich) and 0.03 g Ag_2S powder (99.99%, Aldrich) was placed in an alumina boat after sufficient grinding and then the boat was inserted into the first heating zone of the furnace. Silicon substrates coated with 3 nm Au catalyst were placed at the downstream position with a ~10 cm distance from the CdS source. The reaction chamber was then flushed and filled with a mixture gas of 50 sccm Ar and H_2 (5% in volume) after it was evacuated to a base pressure of 6×10^{-3} Pa. The pressure in the tube was adjusted to 50 Torr before heating. The mixture was then heated up to 850°C and maintained at that temperature for 2 h. After the system cooled to the room temperature, the Si substrates were taken out of the furnace and a layer of yellow wool-like product was observed on their surface. Intrinsic CdS NRs were also synthesized under the same conditions except that Ag_2S powder was not used for comparison.

Morphologies and structures of the as-synthesized CdS:Ag NRs were characterized by X-ray diffraction (XRD, Rigaku D/Max-γB, with Cu Kα radiation), field-emission scanning electron microscopy (FE-SEM, Philips XL 30 FEG), and high resolution transmission electron microscopy (HRTEM, JEM-2010). Compositions of the CdS:Ag NRs were detected by the energy-dispersive X-ray spectroscopy (EDS, attached to SEM).

To assess the electrical and photoconductive properties of the CdS:Ag NRs, back-gate nano-FETs based on individual CdS:Ag NR were constructed. The as-synthesized CdS:Ag NRs were dispersed uniformly onto SiO_2 (500 nm)/p^+-Si substrates at a desired density. And then e-beam evaporation was employed to define the Au (50 nm) electrode on single NR by using a shadow mask consisting of 5 μm thick tungsten wires. Electrical measurements were performed on a semiconductor characterization system (Keithley 4200-SCS) and the white light from the optical microscopy on a probe station was used as the light source to measure the photoconductive properties of the CdS:Ag NRs.

3 Results and discussion

XRD pattern of as-prepared CdS:Ag NRs is shown in Fig. 1. All the diffraction peaks can be indexed to wurtzite

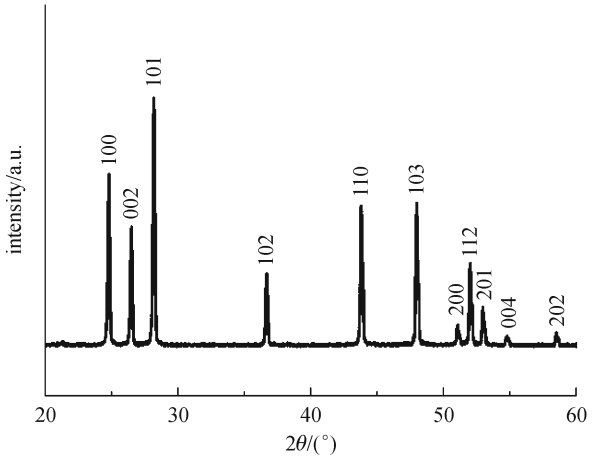

Fig. 1 XRD pattern of as-prepared CdS:Ag NRs

CdS (JCPDS No. 41-1049) and no peaks from the impurities appear, suggesting a high phase purity of the product. Also, we note that no obvious peak broadening or peak shift can be observed for the Ag doped CdS NRs as compared with the undoped ones. This result can be attributed to the fact that the amount of Ag introduced by doping is too little to induce significant lattice distortion of CdS NRs.

Figure 2(a) shows the typical FE-SEM image of the CdS:Ag NRs, from which we can see that the product is composed of a large amount of CdS NRs with very little impurities such as particles. Most of the CdS:Ag NRs have a width in the range of 300–700 nm, a thickness about several tens of nanometers, and a length up to several tens of micrometers. Low-resolution TEM image in Fig. 2(b) further confirms the ribbon-like geometry of the CdS:Ag NRs. It is found that the surfaces of the NRs are smooth and clean and their widths are uniform along the NR length. The atomic ratio of Cd and S estimated from the EDS spectrum (inset in Fig. 2(a)) is about 50.42∶49.58, which is very close to the stoichiometric ratio of CdS. HRTEM image (Fig. 2(c)) and the corresponding selected-area electron diffraction (SAED) pattern (inset in Fig. 2(b)) indicate that the CdS:Ag NRs are single crystals with the [110] growth direction. Lattice spacing of 0.35 and 0.20 nm in the HRTEM image corresponds to the [002] and [110] lattice faces of wurtzite CdS, respectively. All the above-presented results indicate that the crystalline quality and structural integrity of the CdS NRs are not significantly degraded by silver incorporation.

Electrical measurements were performed to determine the doping effects of silver on the transport properties of CdS NRs. The typical *I-V* curves of the silver doped CdS NRs (marked as CA) as well as the intrinsic CdS NRs (marked as C0) measured in dark are plotted in Fig. 3(a). It is noted that the intrinsic CdS NRs have a conductivity as low as $4.3\times10^{-8}\,S\cdot cm^{-1}$, while the conductivity for the silver doped CdS NRs is remarkably

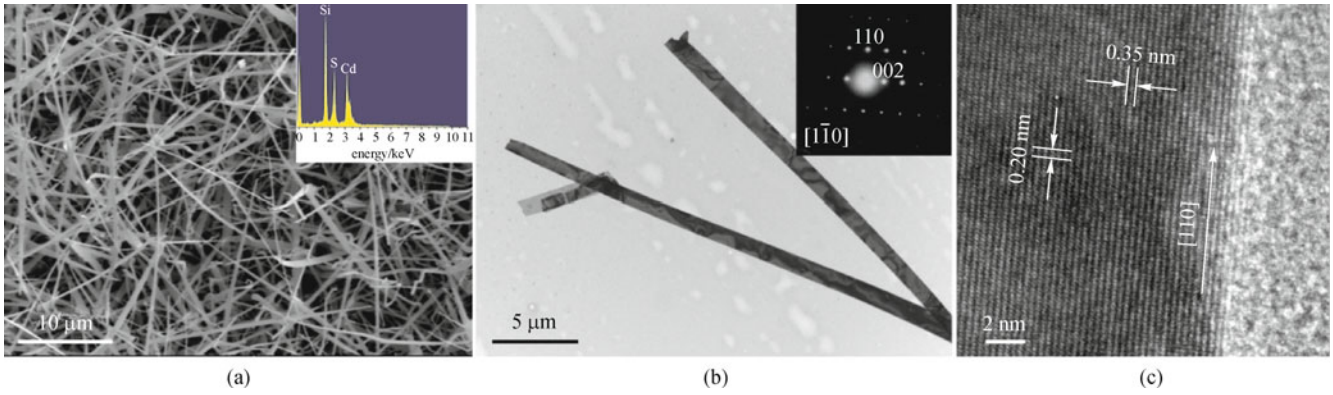

Fig. 2 Morphologies and structures of CdS:Ag NRs. (a) Typical FE-SEM image (inset shows EDS spectrum); (b) low-resolution TEM image (inset shows corresponding SAED pattern); (c) HRTEM image

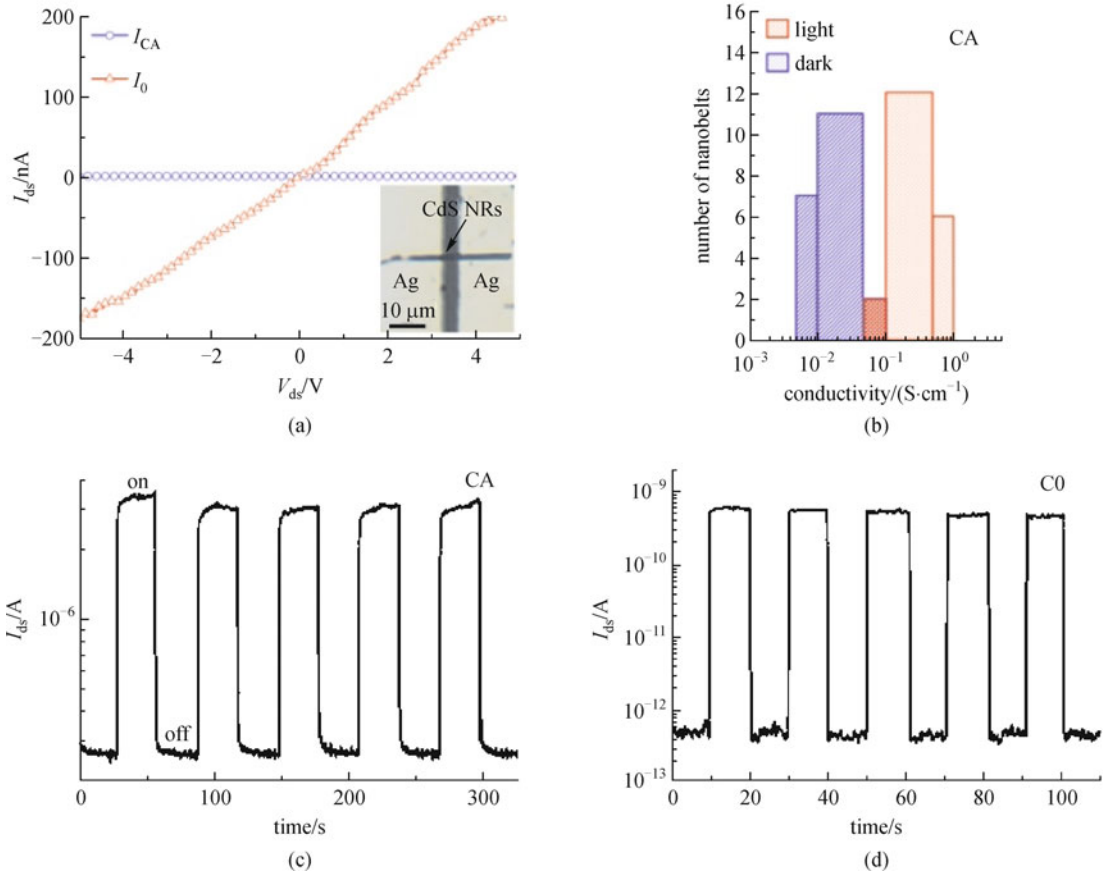

Fig. 3 Electrical and photoconductive properties of CdS:Ag NRs. (a) Typical I_{ds}-V_{ds} curves of CdS NRs (doped and intrinsic) in dark (inset shows photo of typical device based on single CdS:Ag NRs); (b) conductivity distribution of 20 CdS:Ag NRs in dark and upon light illumination; (c) time response of sample CA; (d) time response of sample C0 (LED white light from microscopy was turn on/off manually; V_{ds} was fixed at 5 V)

enhanced to ~3×10^{-2} S·cm^{-1}. Notably, the conductivity of the CdS NRs has been increased ~6 orders of magnitude by Ag doping.

To gain statistical significance, we calculated the conductivity of 20 NRs for CdS:Ag NRs and the corresponding histogram is depicted in Fig. 3(b). It is

seen that the doped CdS NRs have a relative narrow conductivity distribution no matter in dark or upon light illumination. The dark conductivity and photoconductivity are $\sim 5\times10^{-3}-0.1\ \mathrm{S\cdot cm^{-1}}$ and $\sim 0.05-1\ \mathrm{S\cdot cm^{-1}}$, respectively, for the CdS:Ag NRs. Moreover, all the CdS:Ag NRs counted have exhibited an obvious increase in the photoconductivity, verifying the high uniformity of the sample.

Figures 3(c) and 3(d) depict the typical time response spectra of CdS:Ag NRs and undoped CdS NRs, respectively. We note that both the doped and undoped CdS NRs show good photo-response characteristics with excellent stability and reproducibility. The response time of the CdS:Ag NRs is less than 0.5 s, which is comparable to that of the undoped CdS NRs, implying that the CdS:Ag NRs have high crystalline quality with little carrier trapping centers. It is known that the trapping centers induced by the defects play an important role in determining the response speed of the photodetectors [21]. On the other hand, we note that the photocurrent of the CdS:Ag NRs has significantly increased compared to the undoped CdS NRs under the same light intensity, which is 3 μA for CA but only 0.6 nA for C0. Accordingly, the responsivity (R), which represents the current output of a photodetector under light illumination and can be defined as $R\ (\mathrm{A\cdot W^{-1}}) = I_p/P_{opt}$, where I_p is the photocurrent, P_{opt} the incident light power, has increased to $2.7\times10^4\ \mathrm{A\cdot W^{-1}}$ for CA, in contrast to the small value of $5.4\ \mathrm{A\cdot W^{-1}}$ for C0. The enhanced photoconductivity of the Ag doped CdS NRs can be attributed to the increase of the photo-carrier lifetime in the Cd:Ag NRs [22]. In intrinsic CdS NRs, recombination will happen soon after the generation of electron-hole pairs, thus leading to the low photocurrent. In contrast, the holes tend to be trapped in the n-type CdS:Ag NRs, prolonging the lifetime of electrons by preventing the electron-hole recombination. Consequently, the photocurrent is increased since more carriers can pass through the electrodes in a certain time.

The transport properties of the CdS:Ag NRs were further studied by measuring the device characteristics of the bake-gate nano-FET (shown in Fig. 4(a)). Figure 4(b) depicts the typical gate-dependent source—drain current (I_{ds}) versus source-drain voltage (V_{ds}) curves measured at varied gate voltage (V_g) from 0 to 40 V in a step of 10 V. V_g was applied on the degenerated doped Si substrate, which serves as the global back-gate in the nano-FET. It is found that the conductance of the CdS:Ag NR increases with the increase of V_g and tends to be saturated at high V_{ds}, which is inconsistent with the typical behavior of an n-channel metal-oxide-semiconductor FET (MOSFET), revealing the n-type nature of the silver doped CdS NRs. In addition, the electron mobility (μ_n) can be estimated from the channel transconductance (g_m) of the nano-FET, $g_m = \mathrm{d}I_{ds}/\mathrm{d}V_g = (Z/L)\mu_n C_0 V_{ds}$ in the linear regime of I_{ds}-V_g curves, and Z/L is the width-to-length ratio of the NR channel. The capacitance per unit area is given by $C_0 = \varepsilon\varepsilon_0/h$, where ε is the dielectric constant (3.9 for SiO_2), and h is the thickness of the SiO_2 dielectric layer. Based on the above equations, $\mu_n \approx 1.2\ \mathrm{cm^2\cdot V^{-1}\cdot s^{-1}}$ is obtained. Also, the carrier concentration (n_e) is calculated to be $\sim 1.6\times10^{17}\ \mathrm{cm^{-3}}$ from the equation $n_e = \sigma/(\mu_n q)$.

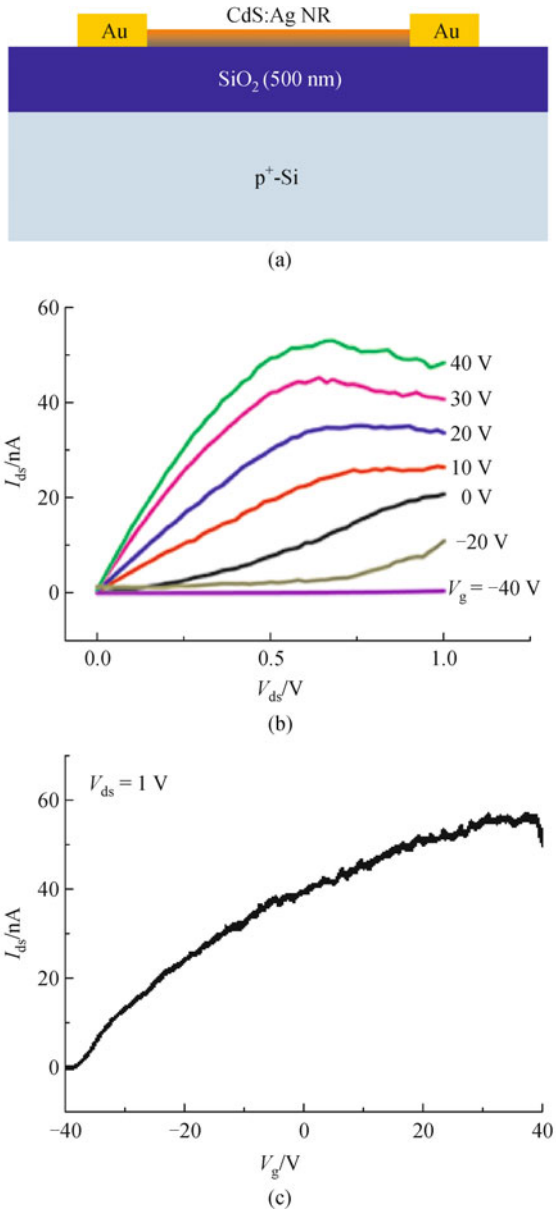

Fig. 4 Transport characteristics of back-gate nano-FET based on CdS:Ag NR. (a) Schematic illustration; (b) I_{ds}-V_{ds} curves measured at varied V_g (V_g increases from 0 to 40 V in a step of 10 V); (c) I_{ds}-V_g curve at V_{ds}= 1 V

According to the previous report [16], there are several different ways for Ag's incorporation into the CdS crystal lattice, including substitution of one Cd^{2+} ion by one or two Ag^+ ions, and incorporation of Ag^+ as an interstitial, etc. Considering the n-type character of the Ag doped CdS NRs, we deduce that the interstitial doping seems to have dominated in this work, i.e., most of Ag^+ act as the interstitial donors in the CdS NRs, which offer free

electrons, and therefore resulting in the enhancement of NR conductivity.

4 Conclusion

In summary, sliver doped n-type CdS NRs were successfully synthesized by using Ag_2S as the dopant via a thermal co-evaporation method. The CdS:Ag NRs had wurtzite single-crystal structure with growth direction of [110]. It was found that the conductivity of the CdS NRs can be increased ~6 orders of magnitude by silver doping, and the photoconductivity was also remarkably enhanced. Furthermore, measurements on the bake-gate nano-FET constructed from single CdS:Ag NR revealed the n-type character of the CdS:Ag NRs. The ability to rationally control the transport properties will greatly promote the practical applications of CdS nanostructures in new-generation nano-optoelectronic devices.

Acknowledgements This work was supported by the National High Technology Research and Development Program of China (No. 2007AA03Z301), the National Natural Science Foundation of China (Grant Nos. 60806028, 20901021), the Program for New Century Excellent Talents in Universities of the Chinese Ministry of Education (No. NCET-08-0764), and the Special Foundation for Doctor of Hefei University of Technology (No. 2007GDBJ028).

References

1. Zheng G F, Lu W, Jin S, Lieber C M. Synthesis and fabrication of high-performance n-type silicon nanowire transistors. Advanced Materials, 2004, 16(21): 1890–1893
2. Huang Y, Duan X F, Lieber C M. Nanowires for integrated multicolor nanophotonics. Small, 2005, 1(1): 142–147
3. Cui Y, Wei Q Q, Park H K, Lieber C M. Nanowire nanosensors for highly sensitive and selective detection of biological and chemical species. Science, 2001, 293(5533): 1289–1292
4. Wang J F, Gudiksen M S, Duan X F, Cui Y, Lieber C M. Highly polarized photoluminescence and photodetection from single indium phosphide nanowires. Science, 2001, 293(5534): 1455–1457
5. Pan Z W, Dai Z R, Wang Z L. Nanobelts of semiconducting oxides. Science, 2001, 291(5510): 1947–1949
6. Liu Y K, Zapien J A, Geng C Y, Shan Y Y, Lee C S, Lifshitz Y, Lee S T. High-quality CdS nanoribbons with lasing cavity. Applied Physicals Letters, 2004, 85(15): 3241–3243
7. Jie J S, Zhang W J, Jiang Y, Meng X M, Li Y Q, Lee S T. Photoconductive characteristics of single-crystal CdS nanoribbons. Nano Letters, 2006, 6(9): 1887–1892
8. Liu Y K, Zapien J A, Shan Y Y, Geng C Y, Lee C S, Lee S T. Wavelength-controlled lasing in $Zn_xCd_{1-x}S$ single-crystal nanoribbons. Advanced Materials, 2005, 17(11): 1372–1377
9. Jie J S, Zhang W J, Bello I, Lee C S, Lee S T. One-dimensional II-VI nanostructures: synthesis, properties and optoelectronic applications. Nano Today, 2010, 5(4): 313–336
10. Duan X F, Huang Y, Agarwal R, Lieber C M. Single-nanowire electrically driven lasers. Nature, 2003, 421(6920): 241–245
11. Wu D, Jiang Y, Wang L, Li S Y, Wu B, Lan X Z, Yu Y Q, Wu C Y, Wang Z B, Jie J S. High-performance CdS:P nanoribbon field-effect transistors constructed with high-*k* dielectric and top-gate geometry. Applied Physics Letters, 2010, 96(12): 123118
12. Jie J S, Zhang W J, Jiang Y, Lee S T. Transport properties of single-crystal CdS nanoribbons. Applied Physics Letters, 2006, 89(22): 223117
13. Gao T, Li Q H, Wang T H. CdS nanobelts as photoconductors. Applied Physics Letters, 2005, 86(17): 173105
14. George P J, Sanchez A, Nair P K, Nair M T S. Doping of chemically deposited intrinsic CdS thin films to n type by thermal diffusion of indium. Applied Physics Letters, 1995, 66(26): 3624–3626
15. Kokaj J, Rakhshani A E. Photocurrent spectroscopy of solution-grown CdS films annealed in $CdCl_2$ vapour. Journal of Physics D: Applied Physics, 2004, 37(14): 1970–1975
16. Ristova M, Ristov M, Tosev P, Mitreski M. Silver doping of thin CdS films by an ion exchange process. Thin Solid Films, 1998, 315 (1–2): 301–304
17. McEvoy A J, Gratzel M. Sensitization in photochemistry and photovoltaics. Solar Energy Materials and Solar Cells, 1994, 32(3): 221–227
18. Wang C Z, E Y F, Fan L Z, Yang S H, Li Y L. CdS-Ag nanocomposite arrays: enhanced electro-chemiluminescence but quenched photoluminescence. Journal of Materials Chemistry, 2009, 19(23): 3841–3846
19. Liu S X, Qu Z P, Han X W, Sun C L. A mechanism for enhanced photocatalytic activity of silver-loaded titanium dioxide. Catalysis Today, 2004, 93–95: 877–884
20. Jia W L, Douglas E P, Guo F G, Sun W F. Optical limiting of semiconductor nanoparticles for nanosecond laser pulses. Applied Physics Letters, 2004, 85(26): 6326–6328
21. He Z B, Jie J S, Zhang W J, Zhang W F, Luo L B, Fan X, Yuan G D, Bello I, Lee S T. Tuning electrical and photoelectrical properties of CdSe nanowires via indium doping. Small, 2009, 5(3): 345–350
22. Soci C, Zhang A, Xiang B, Dayeh S A, Aplin D P R, Park J, Bao X Y, Lo Y H, Wang D. ZnO nanowire UV photodetectors with high internal gain. Nano Letters, 2007, 7(4): 1003–1009